COMPRESSIBILITY EFFECTS ON ROUGHNESS-INDUCED BOUNDARY LAYER TRANSITION

Matteo Bernardini, Sergio Pirozzoli and Paolo Orlandi
Department of Mechanical and Aerospace Engineering
University of Rome 'La Sapienza'
Via Eudossiana 18, 00184, Rome, Italy
matteo.bernardini@uniroma1.it

ABSTRACT

Direct numerical simulation is used to investigate the effect of compressibility on roughness-induced boundary layer transition. Computations are performed in both the low- and the high-speed regime (at free-stream Mach number $M_e = 2$) for an isolated three-dimensional element with cubic shape and for two-dimensional roughness strips. For each configuration two values of the roughness height Reynolds number ($Re_k = 315, 505$) are considered. In the case of 3D roughness, the main effect of the obstacle is the generation of streamwise and wall-normal vorticity, with the formation of an unstable detached shear-layer. Consistent with previous experimental observations, the unsteady release of hairpin vortices past the disturbing element is observed at sufficiently high Re_k for both incompressibile and supersonic flows, which eventually results in the breakdown to turbulence. A major effect of compressibility is observed for two-dimensional roughness, in which case transition is found in the incompressible simulations for both values of Re_k, but only for the higher Re_k under supersonic conditions.

INTRODUCTION

Surface roughness is known to have substantial impact on the aerodynamic performance of aircraft both in the low- and in the high-speed regime, in the case of laminar and turbulent boundary layers. When the incoming boundary layer is laminar, the presence of surface roughness tends to accelerate the laminar-turbulent transition process, which can result in a dramatic increase in drag and aerodynamic heating of the vehicle. Despite their importance in practical applications the physical mechanisms underlying the phenomenon of roughness-induced transition are far from being fully understood. A comprehensive review of the current knowledge of this subject is given by Schneider (2008).

Three-dimensional surface roughness may either occur as discrete, isolated elements (e.g. protruding rivets, or cavities due to impact damage) or as clusters thereof (the so-called distributed roughness), as over an ablating surface. Discrete three-dimensional roughness elements can affect the laminar-to-turbulent transition in a boundary layer in many ways, depending on the size and shape of the roughness element, and many different routes to transition can be identified (Reshotko, 2008). Early experimental observations (Dryden, 1953; Klebanoff *et al.*, 1955; van Driest & McCauley, 1960) suggested that, when the Reynolds number based on the roughness height exceeds a critical value, the transition front begins to move upstream relative to that over a smooth surface. As the height parameter is increased beyond this 'critical' value, the transition location continues to shift upstream until it asymptotes to a location in the near wake of the roughness element (crucially, at a finite distance downstream of the roughness element). Such critical value of the roughness height (for which the element is called 'effective') is influenced by many factors, including the shape of the element, the external disturbance environment and flow compressibility.

A considerable amount of experimental efforts have been spent to determine the transition location as a function of the incoming Reynolds number and the size of the roughness element with respect to the boundary layer thickness. One of the main findings (von Doenhoff & Braslow, 1961; Tani, 1969; Ergin & White, 2006) is that the most significant parameter for the onset of transition in the presence of an isolated three-dimensional roughness is the 'roughness Reynolds number' $Re_k = u(k)k/\nu(k)$, defined in terms of the local flow properties at the edge of the element (of height k) in the undisturbed (laminar) boundary layer. A commonly quoted result is that transition occurs for low-speed flows at $Re_k \approx 500$, if the roughness elements aspect ratio d/k (where d is the spanwise extent of the object) is of order unity.

A correlation to predict the onset of transition in the presence of isolated obstacles was developed by Reshotko & Tumin (2004) for flows over flat plates, as well as in the proximity of blunted leading edges, based on the theory of transient growth. The main result was that the transition Reynolds number based on the local momentum thickness in the absence of the disturbing element (θ) is inversely proportional to the roughness element height, according to

$$Re_{\theta,tr} \sim (k/\theta)^{-1} \, (T_e/T_w)^{-1/2}, \qquad (1)$$

where T_w and T_e are the temperatures at the wall and at the edge of the boundary layer, respectively. Note that, since at

hypersonic speed, $T_w \sim M_e^2$, it follows that

$$Re_{\theta,tr} \sim (k/\theta)^{-1} M_e, \tag{2}$$

which shows that roughness-induced transition is delayed at high Mach numbers, mainly due to the effect of surface heating (Reshotko, 2007). The above correlations have been shown to be in good agreement with experimental data (Reda *et al.*, 2008), and are routinely used in aerospace design. However, since the underlying physical mechanisms are not clearly understood, there is considerable uncertainty in their reliability, which makes it also difficult to extrapolate them to general flow conditions.

Relatively little information is available regarding the flow topology in roughness-induced transition. In particular, the role played by organized vortical structures in generating and sustaining the turbulence cascade process has not been investigated in detail. Early experimental studies (Gregory & Walker, 1956) showed that the flow about an isolated three-dimensional roughness element includes a steady horseshoe vortex that wraps around the obstacle, with two steady counter-rotating vortices trailing downstream. These steady disturbances undergo transient growth, evolving into low- and high-speed streaks. At sufficiently high Reynolds numbers, Acarlar & Smith (1986) showed that unsteady hairpin vortices are shed quasi-periodically from the separated region just downstream of the roughness elements. For moderate Reynolds number ($Re_k \leq 500$), such quasi-periodic disturbances are damped before transition occurs. However, when the Reynolds number becomes large, breakdown to turbulence is observed at a very short, but finite, distance from the roughness element.

In the last decade, the availability of large-scale computing resources has allowed to start studying laminar-turbulent transition by direct numerical simulation (DNS), and examples of calculations of roughness-induced transition have appeared both in the low- and the high-speed case (Rizzetta & Visbal, 2007; Marxen & Iaccarino, 2008). DNS has the advantage of providing detailed information on the flow structure but it requires large computational efforts, and individual studies can cover only a small portion of the large parameter space involved in roughness-induced transition.

In a recent study, Redford *et al.* (2010) have performed DNS of high-speed boundary layers (at $M_e = 3, 6$) over a flat plate with an isolated roughness element consisting of a shallow (high aspect ratio) bump with $k/\delta \approx 0.5$ (δ being the boundary layer thickness). They showed that many features of the transition process are common with the low-speed regime, particularly the lift-up process which follows the generation of streamwise vorticity over the roughness element. Furthermore they found that transition is delayed to higher Reynolds numbers when the Mach number increases, and proposed a correlation to discern laminar from transitional cases.

The objective of the present work is to extend the conditions analyzed in previous investigations, and perform a numerical study of the flow past two- and three-dimensional roughness. In particular for a given roughness element we perform calculations in both the low-and high-speed regime for different values of the roughness Reynolds number. The focus here is on the analysis of disturbances in the near-wake of the element and on the possible influence of compressibility on their evolution.

Table 1. Summary of parameters for DNS study.

Run	M_e	Re_e	Re_k	Transition (?)
M0-3D-315	0	3000	315	N
M0-3D-505	0	5000	505	Y
M2-3D-315	2	10000	315	N
M2-3D-505	2	15000	505	Y
M0-2D-315	0	3000	315	Y
M0-2D-505	0	5000	505	Y
M2-2D-315	2	10000	315	N
M2-2D-505	2	15000	505	Y

NUMERICAL STRATEGY

A strong point of the present work is that for a given geometry of roughness, simulations are performed both in the low- (strictly incompressible) and high-speed (supersonic) regime, thus allowing a one-to-one comparison of the computational results. Owing to the different mathematical character of the incompressible and compressible Navier-Stokes equations, two distinct specifically designed numerical codes are used. Both flow solvers are mainly based on the concept of preservation of kinetic energy at the discrete level through suitable discretization of the convective terms, which yields stable numerical solutions without reverting to any form of spurious numerical dissipation. In our opinion this is a mandatory pre-requisite for numerical calculations of transitional flows to be reliable, since spurious numerical dissipation could artificially impact the evolution of the localized disturbances generated by the roughness element, thus preventing or delaying the (possible) breakdown to turbulence.

The incompressible Navier-Stokes equations are solved by means of a second-order finite-difference code based on staggered discretization of the flow variables and a third-order Runge-Kutta scheme for time integration. In this case the roughness element is handled through the immersed boundary method, which allows simple and effective coupling with the flow solver. The details of the implementation can be found in Orlandi & Leonardi (2006), and the application of the code to the study of fully turbulent and transitional flow in a rough channel is reported in Orlandi & Leonardi (2008) and Orlandi (2009).

The flow solver for the compressible calculations relies on sixth-order central discretization of the convective terms of the Navier-Stokes equations cast in split form (Pirozzoli, 2010), and it allows for the capture of shock waves (if any) by means of localized application of high-order WENO numerical reconstructions controlled by the Ducros shock sensor (Pirozzoli *et al.*, 2010). The diffusive terms are expanded to Laplacian form for improved stability, and approximated

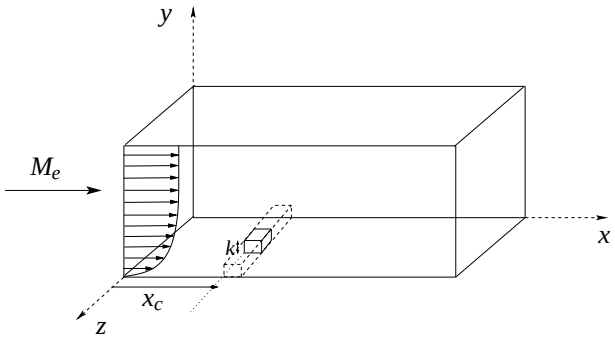

Figure 1. Sketch of the computational arrangement used for DNS of transition past three-dimensional (solid lines) and two-dimensional (dashed lines) obstacles.

with sixth-order central difference formulas. The resulting semi-discrete ODE system is integrated in time with an explicit fourth-order Runge-Kutta algorithm. In this case the computational grid is constructed so as to match the shape of the roughness element.

A schematic representation of the computational arrangement used for the simulation is reported in Fig. 1. The domain includes the roughness element (at a distance x_c from the inlet) which perturbs an initially laminar boundary layer over a flat plate, whose shape is determined from the solution of the generalized Blasius equations (White, 1974), with the assumption of adiabatic wall. In all cases, random velocity disturbances whose maximum amplitude is approximately 1% of the free-stream velocity u_e are also enforced at the inflow to stimulate boundary layer transition. At the top and outflow boundaries radiative boundary conditions are prescribed and periodicity is exploited in the spanwise direction. In the supersonic cases the temperature of the no-slip wall is set to the value corresponding to adiabatic conditions.

The computational domain extends for $L_x = 25.55\,\delta$, $L_y = 10\,\delta$, $L_z = 3.2\,\delta$ in the streamwise (x), wall-normal (y) and spanwise (z) directions, where δ (the boundary layer thickness at the inflow station) is chosen as the reference length for normalization. The domain is discretized with a grid consisting of $N_x = 512$, $N_y = 101$ $N_z = 128$ points, which are equally spaced in x and z directions, and clustered to the wall according to a hyperbolic sine mapping function. A grid sensitivity study was preliminarily performed to assess the independence of the results from the mesh resolution.

The roughness elements considered in the present work belong to two classes: an isolated three-dimensional obstacle with cubic shape, and a two-dimensional roughness strip with square cross section. The height of the elements is the same ($k = 0.25\,\delta$) and both are placed at a distance $x_c = 5.1\delta$ from the inlet station. Simulations have been performed for free-stream Mach number $M_e = 0$ and $M_e = 2$ for two values of the roughness Reynolds number, $Re_k = 315, 505$, for a total of eight simulations, all listed in Tab. 1.

RESULTS

Due to the surface heating experienced by a wall-bounded supersonic flow, the thermodynamic properties are not uniform across the wall layer, resulting in a low-density, high-temperature region close to the wall, where the molecular viscosity is reduced with respect to the free stream (approximately by a factor of two at the Mach number here considered). As a consequence, when compared with an incompressible boundary layer at the same outer Reynolds number $Re_e = u_e\delta/\nu_e$, a high-speed boundary layer is dominated by high levels of viscous dissipation in the wall region, and as a consequence it is less prone to be tripped by roughness elements (Schneider, 2008). This is the primary (obvious) effect of compressibility on the boundary layer transition, which was preliminarily verified by performing a series of supersonic simulations (not reported here) at the same outer Reynolds number as the incompressible cases reported in Tab. 1. As expected, the obstacle does not cause any sizeable modification of the boundary layer structure under supersonic conditions, and the disturbance introduced by roughness dies out immediately downstream of the element. Another obvious effect on the global flow structure is the onset of a pattern of expansions and shock waves in the free-stream due to the interaction of the obstacle with the incoming stream. However, due to the relatively small height of the elements the external wave pattern (not shown) is found to be rather weak in all cases here analyzed, and it is not expected to affect the transition process.

Since the roughness Reynolds number is expected to be the fundamental parameter governing transition, it is more interesting to look for more subtle compressibility effects, by performing comparisons at the same value of Re_k. Being the height of the roughness element constant between the various cases, this implies the need to increase the outer Reynolds number in supersonic simulations. A preliminary overview of the computational results can be gained from Tab. 1, where an indication of the flow condition far from the roughness location (transition to turbulence or not) is provided for each simulation in the last column. Consistent with previous experimental observations, in the case of the three-dimensional cubic element, transition does not occur when the roughness Reynolds number is small (below $Re_k \approx 500$), for both low- and high-speed boundary layers. Note that the present results suggest a value of the critical Reynolds number ($Re_{k,tr} \approx 500$) which is consistent with typical values reported in literature for isolated elements of similar aspect ratio (Ergin & White, 2006). On the other hand, in the case of two-dimensional roughness strips, the breakdown to turbulence is found for both the incompressible simulations, but only for the higher Reynolds number in the supersonic case.

A visual perception of the flow organization in the present simulations is provided by Fig. 2, where instantaneous iso-surfaces of the 'swirling strength', which effectively characterizes tube-like vortex structures, (Zhou *et al.*, 1999)) are shown for representative flow cases, coloured by the local value of the streamwise velocity. In the case of three-dimensional roughness the main flow feature is the unsteady release of hairpin vortices which propagate downstream of the element forming packets (Adrian *et al.*, 2000), and giving rise to a turbulent spot by the end of the computational domain. This mechanism appears to be similar at both low and high-speeds, and it resembles the hydrogen-bubble-wire visualizations of the flow past an hemispherical obstacle (Acarlar & Smith, 1986). In analogy with that experiment a necklace vortex wrapping around the obstacle (the so-called standing

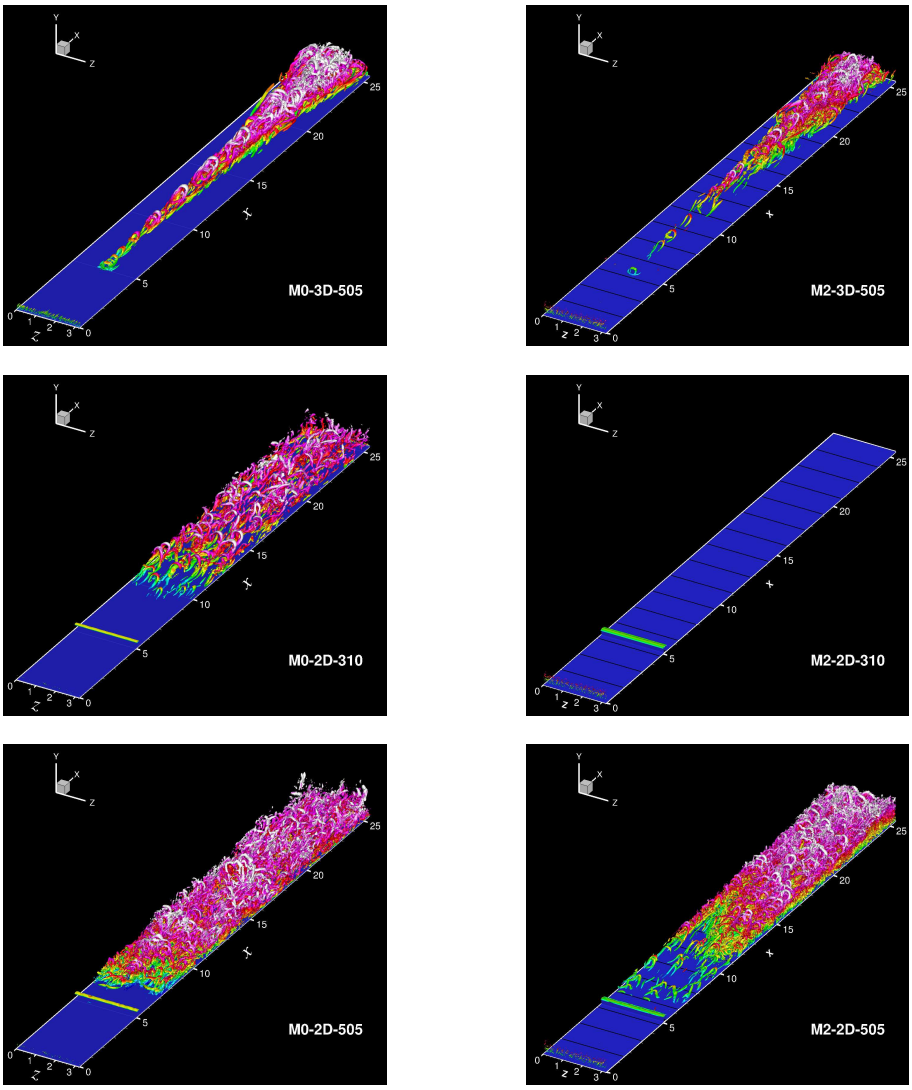

Figure 2. Three-dimensional view of coherent structures for some representative flow cases. Iso-surfaces of vortex tubes strength are shown, coloured by the local value of the streamiwse velocity.

vortex) is also observed (see Fig. 3). Clearly, the details of the flow pattern in the proximity of the obstacle are strongly dependent on the its shape, and for instance the standing vortex is not observed for smooth bump-shaped obstacles (Redford *et al.*, 2010). The formation of hairpin vortices is usually explained by invoking the lift-up mechanism of low-speed fluid past the obstacle, with the associated generation of a detached shear layer, which is shown in a cross-stream plane in the near wake of the element in Fig. 4 for a representative case. The intrinsic instability associated with the inflectional points of the velocity profiles past the element causes roll-up of vorticity by an inviscid Kelvin-Helmholtz type mechanism and the shedding of hairpins vortices, which play the major role in the breakdown to turbulence. Furthermore, a 3D element also gives rise to lateral shear layers having strong wall-normal vorticity, as shown in Fig. 4, which can have an important influence on the breakdown mechanism (Andersson *et al.*, 2001). In the 3D element case the magnitude of ω_y is found to be of the same order as ω_z, in contrast with the findings for a shallow bump, which is less effective in generating wall-normal vorticity (Redford *et al.*, 2010), This scenario is found to be similar for both incompressible and supersonic flow cases.

The effect of two-dimensional roughness on the vorticity dynamics is markedly different (Klebanoff *et al.*, 1992). At least at low speed, it is believed that two-dimensional roughness is more effective in inducing transition, and the transition point moves upstream more gradually with increasing Re_k. This can be appreciated from the present (incompressible) data from both the visualizations of Fig. 2 and (more quantitatively) from the distribution of the spanwise-averaged skin friction coefficient displayed in Fig. 5. Conventionally assuming as transition point the streamwise location where the skin friction starts to increase sharply, it is clear that transition is shifted upstream at higher Re_k. This behaviour can be interpreted regarding two-dimensional roughness strips as gen-

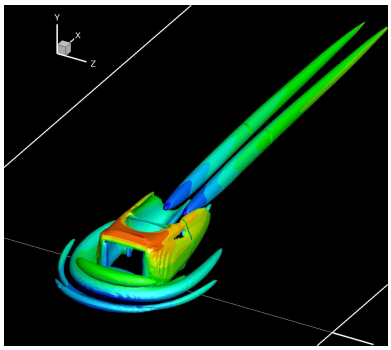

Figure 3. Zoom of the vortical structures around the obstacle showing the formation of the standing vortex (run M0-3D-505).

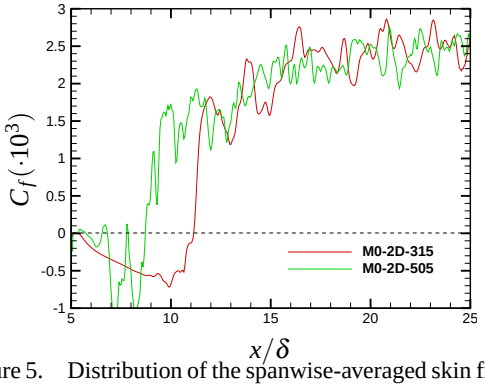

Figure 5. Distribution of the spanwise-averaged skin friction coefficient for incompressible cases with 2D roughness.

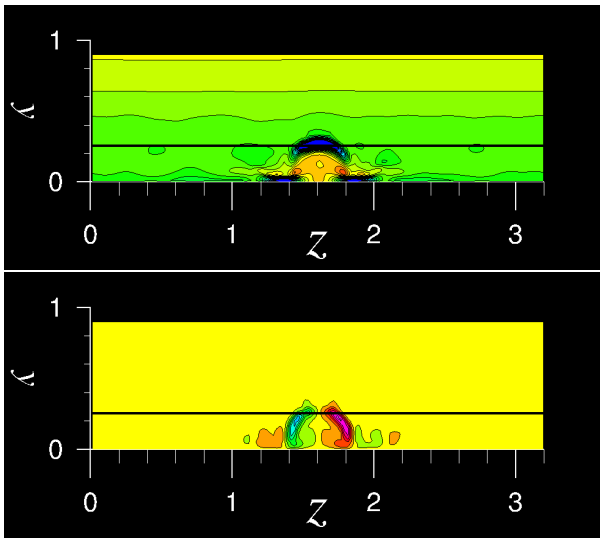

Figure 4. Contours of spanwise (top) and wall-normal (bottom) vorticity component for case M0-2D-505 at $x/\delta = 15.5$.

erators of Tollmien-Schlichting waves (Ergin & White, 2006), whose increasing amplitude is expected to shift the transition location toward the roughness element. In this context one can attempt to explain why the supersonic boundary layer at the lower Reynolds number (test M2-2D-315) does not show transition to turbulence. At low supersonic Mach numbers (below $M_e = 4$) the two-dimensional boundary layer linear stability theory predicts that, unlike in incompressible flow, the most amplified modes are three-dimensional, consisting of oblique waves (Mack, 1984; Malik, 1989). The different behaviour observed for cases M0-2D-315 and M2-2D-315 should then be tentatively ascribed to the effect of compressibility, which makes supersonic streams less effective in amplifying the two-dimensional disturbances induced by the roughness element.

CONCLUSIONS

The influence of compressibility in roughness-induced transition has been investigated through direct numerical simulations in both the low- and the high-speed regime for two-dimensional and three-dimensional roughness elements. For the flow conditions here analyzed, major effects of compressibility are not observed in the case of cubic obstacles, both in terms of flow topology and of critical roughness Reynolds number, which is found to be $Re_{k,tr} \approx 500$, in agreement with the argument (Ergin & White, 2006) that Re_k should be the controlling parameter in the case of small roughness elements. The main effect of the obstacle is the generation of shear layers which, at sufficiently high values of Re_k result in the shedding of hairpin vortices and breakdown to turbulence. In the case of two-dimensional roughness strips differences arise between the incompressible and the compressible regime. Specifically, supersonic boundary layers appear to be less effective in amplifying two-dimensional disturbances generated by the obstacle, and transition is not observed at the lower Re_k here considered.

Given the limited number of simulations performed so far, no conclusive statements on the influence of the flow parameters on the transition process can be made. In particular, additional efforts are required to establish the effect of changes in the external disturbance environment and of as of the obstacle height. Simulations at higher Mach number for both two-dimensional and three-dimensional roughness elements would also be revealing to better elucidate genuine compressibility effects on the boundary layer transition.

ACKNOWLEDGMENTS

We acknowledge CINECA and CASPUR for the availability of high-performance computing resources.

REFERENCES

Acarlar, M. S. & Smith, C. R. 1986 A study of hairpin vortices in a laminar boundary layer. part 1. hairpin vortices generated by a hemisphere protuberance. *J. Fluid Mech.* **175**, 1–41.

Adrian, R. J., Meinhart, C. D. & Tomkins, C. D. 2000 Vortex organization in the outer region of the turbulent boundary layer. *J. Fluid Mech.* **422**, 1–54.

Andersson, P., Brandt, L., Bottaro, A. & Henningson, D.S. 2001 On the breakdown of boundary layer streaks. *J. Fluid Mech.* **428**, 29–60.

von Doenhoff, A.E. & Braslow, A.L. 1961 Effect of distributed surface roughness on laminar flow. In *Boundary Layer and flow Control* (ed. G. V. Lachmann), , vol. 2. Pergamon.

van Driest, E. R. & McCauley, W. D. 1960 Measurements of the effect of two-dimensional and three-dimensional roughness elements on boundary layer transition. *J. Aero. Sci.* **27**, 261–271.

Dryden, H. 1953 Review of published data on the effect of roughness on transition from laminar to turbulent flow. *J. Aeronaut. Sci.* **20**, 477–482.

Ergin, F. G. & White, E. B. 2006 Unsteady and transitional flows behind roughness elements. *AIAA J.* **44**, 2504–2514.

Gregory, N. & Walker, W. S. 1956 The effect of transition of isolated surface escrescences in the boundary layer. *Tech. Rep.* R & M 2779. Aero. Res. Council Tech. Report.

Klebanoff, P., Cleveland, W. & Tidstrom, K. 1992 On the evolution of a turbulent boundary layer induced by a three-dimensional roughness element. *J. Fluid Mech.* **237**, 101–187.

Klebanoff, P., Schubauer, G. & Tidstrom, K. 1955 Measurements of the effect of two-dimensional and three-dimensional roughness elements on boundary layer transition. *J. Aero. Sci.* **22**, 803–804.

Mack, L.M. 1984 Boundary-layer linear stability theory. Agard rep. 709. Spec. Course Stab. Transit. Laminar Flows.

Malik, M.R. 1989 Prediction and control of transition in supersonic and hypersonic boundary layers. *AIAA J.* **27**, 1487–1493.

Marxen, O. & Iaccarino, G. 2008 Numerical simulation of the effect of a roughness element on high-speed boundary-layer instability. AIAA paper 2008-4400. 38^{th} Fluid Dynamics Conference and Exhibit, Seattle, WA.

Orlandi, P. 2009 Rough channels. In *Proc. TSFP-6: turbulence and shear flow phenomena*. Seoul, Corea.

Orlandi, P. & Leonardi, S. 2006 DNS of turbulent channel flows with two- and three-dimensional roughness. *J. of Turbulence* **7**.

Orlandi, P. & Leonardi, S. 2008 Direct numerical simulation of three-dimensional turbulent rough channels: parameterization and flow physics. *J. Fluid Mech.* **606**, 399–415.

Pirozzoli, S. 2010 Generalized conservative approximations of split convective derivative operators. *J. Comput. Phys.* **229**, 7180–7190.

Pirozzoli, S., Bernardini, M. & Grasso, F. 2010 Direct numerical simulation of transonic shock/boundary layer interaction under conditions of incipient separation. *J. Fluid Mech.* **657**, 361–393.

Reda, D. C., Wilder, M. C., Bogdanoff, D. W. & Prabhu, D. K. 2008 Transition experiments on blunt bodies with distributed roughness in hypersonic free flight. *J. Spacecraft and Rockets* **45**, 210–215.

Redford, J.A., Sandham, N.D. & Roberts, G.T. 2010 Compressibility effects on boundary-layer transition induced by an isolated roughness element. *AIAA J.* **48**, 2818–2830.

Reshotko, E. 2007 Is Re_θ/M_e a meaningful transition criterion? *AIAA J.* **44**, 1441–1443.

Reshotko, E. 2008 Transition issues for atmospheric entry. *J. Spacecraft and Rockets* **45**, 161–164.

Reshotko, E. & Tumin, A. 2004 Role of transient growth in roughness-induced transition. *AIAA J.* **42**, 766–770.

Rizzetta, D.P. & Visbal, M.R. 2007 Direct numerical simulations of flow past an array of distributed roughness elements. *AIAA J.* **45**, 1967–1976.

Schneider, S.P. 2008 Effects of roughness on hypersonic boundary-layer transition. *J. of Spacecraft and Rockets* **45**, 193–209.

Tani, I. 1969 Boundary layer transition. *Annu. Rev. Fluid Mech.* **1**, 169–196.

White, F. M. 1974 *Viscous fluid flow*. McGraw-Hill, New York.

Zhou, J., Adrian, R. J., Balachandar, S. & Kendall, T. M. 1999 Mechanisms for generating coherent packets of hairpin vortices in channel flow. *J. Fluid Mech.* **387**, 353–396.